Journal of Oil Palm Research
DOI: https://doi.org/10.21894/jopr.2022.0068

EXPLORING SENTINEL-2 SATELLITE IMAGERY-BASED VEGETATION INDICES FOR CLASSIFYING HEALTHY AND DISEASED OIL PALM TREES

NARISSARA NUTHAMMACHOT[1]* and DIMITRIS STRATOULIAS[2]

ABSTRACT

*The cultivation of oil palm (*Elaeis guineensis *Jacq.) trees is one of the most important agricultural activities and a major sector of economic development in Thailand. However, oil palm trees are susceptible to diseases that can decrease the profitability of the business. Decreasing productivity sometimes triggers an expansion of the cultivated area, which is often negatively affecting surrounding natural habitats. Remote sensing technology has increasingly been used for investigating, detecting and mapping plant related traits. This study aims to use concurrently acquired Sentinel-2 satellite imagery, Unmanned Aerial Vehicle (UAV) field survey and ground observation data to identify the characteristics of oil palm trees based on three controlled sites (namely healthy, diseased and mixed oil palm tree areas). The GNDVI, NDVI, NDI45, RVI, MSAVI and MTCI vegetation indices (VI) were used as a predictor of plant biomass and indicator of oil palm tree disturbance. A linear regression model was applied to each of the derived VIs to determine the index with the strongest relationship to biomass for each of the three sites. The outcome of this study showed; (1) that the most effective indicators were NDVI for the healthy oil palm area and RVI index for the diseased oil palm area (R^2 = 0.48 and 0.68, respectively), and (2) the MSAVI provided the best R^2 value in patterns correlated to the greenness of vegetation for the mixed oil palm tree areas (R^2 = 0.44). Moreover, the results show that the overall Support Vector Machine (SVM) classification accuracy is 72.97%, with the kappa coefficient is 0.56 for the healthy oil palm area, 64.16% and 0.40 for the diseased oil palm area and 50.00% and 0.37 for the mixed oil palm area. A concurrent UAV survey based on the visible and Visible Atmospherically Resistant Index (VARI) bands and SVM classification provided higher overall accuracy compared to the Sentinel-2 SVM classification.*

Keywords: oil palm diseases, Sentinel-2 Support Vector Machine (SVM) classification, Unmanned Aerial Vehicle (UAV), vegetation indices.

Received: 25 January 2022**; Accepted:** 8 August 2022**; Published online:** 19 October 2022.

INTRODUCTION

Oil palm has been a major Southeast Asian agricultural commodity, with an essential economic contribution especially in the south of Thailand. However, many diseases such as the *Ganoderma boninense* have considerably infected oil palm crops in different regions (Naher *et al.*, 2013). The early identification of diseases is an important first step to controlling and preventing potential outbreaks and decreasing the environmental effect of agrochemicals and economic losses. The traditional methods to halt outbreaks and to detect symptoms inherit have several disadvantages such as the fact that they are time consuming and labour intensive. Therefore, the application of satellite and aerial remote sensing has been widely used to identify automatically oil palms, map the extent and estimate the yield (Cheng

[1] Faculty of Environmental Management, Prince of Songkla University, Hatyai, Songkhla 90110, Thailand.

[2] Asian Disaster Preparedness Center, 24th Floor, SM Tower, 979/69-70 Paholyothin Road, Phyathai, Bangkok 10400, Thailand.

* *Corresponding author e-mail: narissara.n@psu.ac.th*

et al., 2018; 2019; Chong *et al.,* 2017; Yusoff *et al.,* 2017). Remote sensors can detect the energy from the spectral reflection of plants, based on which, the condition of the oil palm leaf can be assessed. Principally the spectral information from the satellite data associates with the biophysical properties of the crops. Several studies have shown that multispectral remote sensing data can discriminate between healthy and diseased oil palm trees. For instance, Malinee *et al.* (2021) detected oil palm disease in Krabi Province, Thailand using a WorldView-2 satellite image with an overall maximum likelihood classification accuracy of 85.98% and kappa coefficient of 0.71.

Santoso *et al.* (2011) selected QuickBird imagery to identify and map basal stem rot disease in oil palms. All the vegetation indices showed different accuracy from diverse palm age fields. The accuracy performance for 15 and 18 year old oil palms was only 35% while in the fields of 10 and 21 year old palms with an accuracy of 62% and 67% respectively were estimated. Santoso *et al.* (2017) mapped Basal Stem Rot (BSR) disease in oil palms using QuickBird imagery. They found that the Random Forest (RF) model performed the best at predicting, classifying, and mapping oil palm trees.

Izzuddin *et al.* (2018) used the airborne hyperspectral image for detecting *Ganoderma* disease in oil palm trees. Five VIs were selected in this study. The VI provided low to moderate percentages (30%-40%) of accuracy classification for oil palm disease. Kamal *et al.* (2018) classified leaf disease symptoms of oil palm trees. A SVM algorithm was applied for *Chimaera* and *Anthracnose* diseases classification. The SVM classification accuracy for *Chimaera* was 97% while the accuracy for *Anthracnose* was 95%. With regard to the classification algorithm, SVM is a non-parametric classifier with increasing popularity and application in remote sensing. SVM has been applied on remotely sensed data in crop related studies and proved useful as they provide high classification accuracy (Chaware *et al.,* 2017; Kamal *et al.,* 2018; Masazhar *et al.,* 2017).

For the above reasons, the SVM classification algorithm was selected for classified healthy and diseased oil palm plants in the current study which deals with the problem of discriminating between diseased and healthy oil palm trees based on the high-resolution multi-spectral image. Therefore, a novel algorithm is suggested. The model of the proposed method is to use the VI with the highest discriminatory power in distinguishing between diseased oil palm and healthy oil palm objects. The proposed method is useful because some VI cannot give good results from certain satellite images and have limited robustness. For example, NDVI indices cannot identify the true phenology of plants because the radiometric information cannot be computed.

The objectives of the current paper are (i) to investigate the correlation of popular VIs by demonstrating the discriminatory power between diseased and healthy oil palm trees, (ii) to detect the plant diseases in oil palms based on Sentinel-2 satellite imagery, (iii) to compare the accuracy of SVM classification when applied on Sentinel-2 satellite and Unmanned Aerial Vehicle (UAV) images, and (iv) to validate two sample data groups Visible Atmospherically Resistant Index (VARI) of UAV and VARI of Sentinel-2 data using regression modelling. The results from this study can be beneficial for developing disease management programmes and infection monitoring systems.

MATERIALS AND METHODS

Study Area

The study area is situated in Chana district, Songkhla province, Thailand which is located around the geographical coordinates 6° 54′ 51″ N and 100° 44′ 26″ E as depicted in *Figure 1*. The climate of southern Thailand is characterised by a rainy season which lasts from May to January of the following year. The average annual temperature is approximately 26.8°C and the average annual rainfall is 1622 mm. These conditions are suitable for the cultivation of oil palm which is the dominant plantation crop in the greater area. The areas sampled were characterised by flat terrain and commercial oil palm plantations with no nutrient deficiencies and pest infestation.

Field Data Collection

Both diseased and healthy oil palm tree samples were selected based on random sampling on the same day (12th June 2020). In study area 1 (healthy oil palm trees), the age of the trees was 5 years and 50 points were selected, in study area 2 (diseased oil palm trees), the age of the trees was 13 years, and 55 points were selected and in study area 3 (mixed diseased and healthy oil palm trees), the age of the trees was 15 years and 100 points were collected. These collected points were described and depicted as point data in *Figure 2.* The distance between oil palm trees was approximately 9 m for all sites. The geopositioned of the tree points were recorded with a Global Navigation Satellite System (GNSS) device and the health status of each oil palm was inspected and evaluated by an experienced farmer. A random selection of 70% of reference points was used as training data for classification and the remaining 30% of samples were used as the validation data for each site. Furthermore, a UAV was used to fly over and acquire images of these areas for validation purposes. DroneDeploy software (14 day trial version) was used to mosaic the images collected and analyze tree health (*Figure 2).* The UAV flew at an altitude of approximately 50 m and covered the entire area.

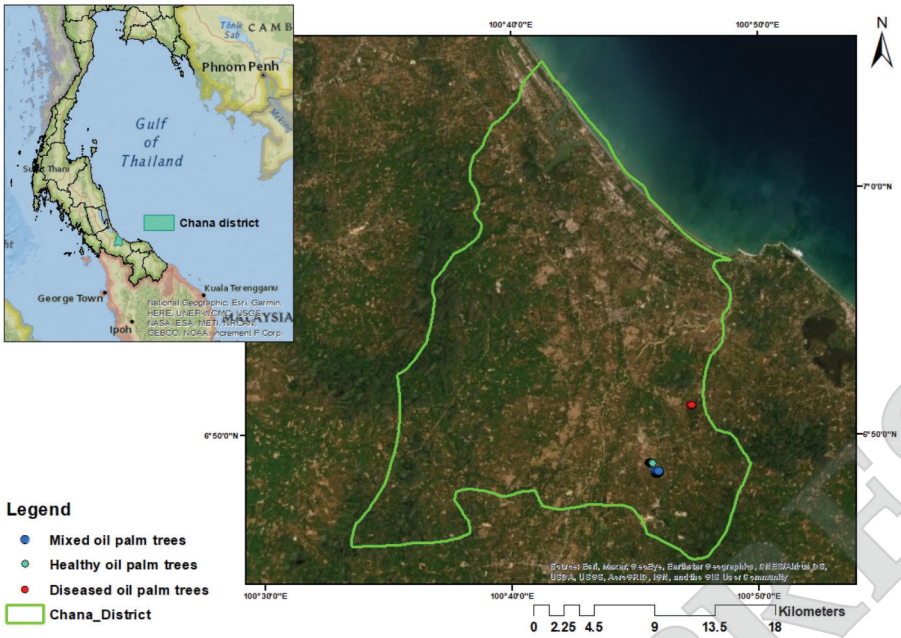

Figure 1. Location of the oil palm planted areas in Chana district, Songkhla province, Thailand.

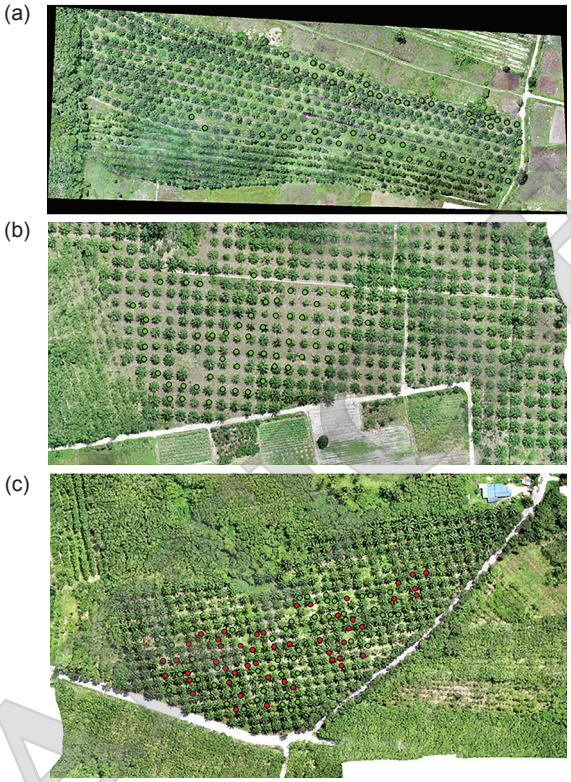

Note: Red point - diseased oil palm; Green point - healthy oil palm.

Figure 2: Sample points of each area and the photos from the UAV (a) healthy oil palm sample points and UAV image, (b) diseased oil palm sample points and UAV image, (c) mixed oil palm sample points and UAV image.

Unmanned Aerial Vehicle (UAV)

A DJI Phantom 4 Pro quadcopter (Da-Jiang Innovations (DJI), China) was used during the survey flights to capture RGB images. The internal RGB device camera uses a Sony 1" complementary metal-oxide-semiconductor (CMOS) sensor with 20M effective pixels. The embedded GNSS and a navigation control system ascribe high positional accuracy and stable flight characteristics to the platform (DJI, 2017).

Data acquisition. Three inspections were carried out over healthy, disease and mix (healthy and diseases) oil palm planted areas. The date, 12th June 2020 was selected, with a clear sky and no rain. For the healthy oil palm tree site, the entire area was covered with 160 images acquired at 48.768 m altitude. Likewise, the diseased oil palm tree and mixed oil palm tree sites covered an area of 0.0627 and 0.2300 km^2 respectively; 154 and 142 images were collected at 51.816 and 51.816 m altitude, respectively. The spatial resolution of the UAV images was approximately 50 mm. Based on visual interpretation of the UAV high spatial resolution images, oil palm trees were recognised by visible symptoms of the disease manifestation. However, the mixed oil palm planted area showed a slightly different in their appearance. More details regarding each site and flight conditions are presented in *Table 1.*

Data processing and analysis. The RGB imagery datasets were processed using the DroneDeploy software. The workflow was implemented with the following major steps: i) plan a mapping flight and fly; ii) upload images; iii) mosaic images; iv) export images. Further processing was carried out in SNAP software version 6.0. The VARI was adjusted to the RGB data as in Equation (1). VARI is used to

TABLE 1. AERIAL PHOTOS CAPTURED BY DJI PHANTOM 4 PRO AT EACH SITE

Site	Date	Images Collected	Area (km^2)	Age of oil palm tree (years)	The average height of oil palm trees (m)	UAV flight altitude (m)
Healthy oil palm tree	12th June 2020	160	0.0672	5	4.0	48.768
Diseased oil palm tree	12th June 2020	154	0.0627	13	7.5	51.816
Mixed oil palm tree	12th June 2020	142	0.2300	15	11.0	51.816

evaluate the fraction of vegetation in a scene with low sensitivity to atmospheric effects. It is suitable for monitoring low-altitude drone imagery (ESRI, 2021).

$$VARI = \frac{Green - Red}{Green + Red - Blue} \quad (1)$$

A supervised classification approach was adopted to classify the RGB and VARI bands of the drone imagery in each site using the QGIS software and based on 5 classes namely disease, healthy, forest, road and others.

Sentinel-2 Data Collection and Pre-processing

An image from the Sentinel-2B satellite launched on 7th March 2017 is used in this study. The data are available and can be downloaded from the European Space Agency (ESA) website (https://sentinel.esa.int) (ESA, 2021). The Sentinel-2B satellite carries the high quality Multispectral Instrument (MSI) capable of recording information in 13 spectral bands at 3 nominal spatial resolutions (visible (VIS) – Near Infrared (NIR) bands at 10 m, red-edge, narrow NIR and SWIR bands at 20 m, and three bands (Coastal aerosol, Water Vapor, and Cirrus) at 60 m spatial resolution) (ESA, 2015). The Sentinel-2 mission has 10 day revisit frequency at the equator with one satellite and 5 days with 2 satellites under cloud-free conditions which results in 2-3 days at mid-latitudes. The Sentinel-2B image was acquired on 25 June 2020 and provided a clear image of the study area. It was downloaded at level-1C (Top of Atmosphere) with 13 spectral bands. We selected an image in June (25th June 2020) based on the condition of disease and non-disease oil palm trees. The Sentinel Application Platform (SNAP), free software developed by ESA, was used to pre-process the data and calculate the related spectral indices. Pre-processing of the Sentinel-2 image was spatially re-sampled and subset to the area of interest. The spectral reflectance of bands B3 (Green)-B8A (NIR) was used to predict the vegetation indices estimation. Ten bands (B2-B8A, B11 and B12) were selected to classify the images.

Methodology

Radiometric correction. A clear and cloud-free Sentinel-2 image with 13 spectral bands acquired on 25th Jun 2020 was downloaded at level 1C Top of Atmosphere (TOA) reflectance. L1C data is not atmospherically corrected, therefore the Atmospheric Rayleigh Scattering Correction was selected to convert to Bottom of Atmosphere (BOA) reflectance.

Geometric correction. Level-1C processing includes ortho-rectification and spatial registration on a global reference system with sub-pixel accuracy. The next step of the pre-processing was to do resampling process. This process was done to change spatial resolution images. All images were resampled to 10 m spatial resolution using the nearest neighbour method. The images were subset around the selected three areas of interest to computationally speed up the process.

Vegetation indices. The multispectral bands of visible and NIR were estimated for vegetation indices (Askar *et al.*, 2018). In this study, we used the NIR, Red and Green bands to calculate all indices using the SNAP software version 6.0. The formulas of the vegetation indices selected are presented in *Table 2*. In order to assess the accuracy of the indices, the statistical distributions of the healthy and diseased oil palm tree classes were investigated. The scattering correlation plots between the VARI of UAV and all indices of Sentinel-2 spectral values were calculated. Linear regression was selected to estimate the best parameters from Sentinel-2 satellite data. The coefficient of determination or R^2 indicates that the regression model is in fit performance.

Support Vector Machine (SVM) Classification

Diseased and healthy oil palm trees maps in each area were classified from the Sentinel-2 and UAV images with the SVM classification algorithm. The Sentinel-2 image pattern was classified on 10 bands composite and based on visual interpretation. The Sentinel-2 image from the diseased oil palm planted area was classified into diseased oil palm trees, forest, road and others while the UAV image was classified as diseased oil palm trees, forest, background, road and others. Sentinel-2 image from healthy oil palm trees area was classified into healthy oil palm trees, forest, road and others

TABLE 2. THE VEGETATION INDICES AND MATHEMATICAL FORMULAS USED IN THIS STUDY

Indices	Formula	Reference
Green normalised difference vegetation index (GNDVI)	(NIR − GREEN)/(NIR + GREEN)	Gitelson *et al.* (1996)
Normalised difference vegetation index (NDVI)	(NIR − RED)/(NIR + RED)	Tucker (1979)
The normalised difference index (NDI45)	(NIR-RED)/(NIR+RED) Where NIR = B5 and RED = B4	Delegido *et al.*(2011)
The ratio vegetation index (RVI)	RVI = (NIR/RED)	Zhang *et al.* (2021)
The modified soil adjusted vegetation index (MSAVI)	(2 * NIR + 1 – sqrt ((2 * NIR + 1)^2 – 8 * (NIR - R))) / 2	Qi *et al.* (1994)
The meris terrestrial chlorophyll index (MTCI)	(NIR-RED2)/(RED2-RED1) Where NIR = B6, RED2 = B5, RED1 = B4	Pałaś *et al.* (2020)

while UAV was classified to healthy oil palm trees, forest, background, road and others. For mixed oil palm planted area, it was classified into 5 categories namely diseased oil palm trees, healthy oil palm trees, forest, road and others for satellite data while it was classified into diseased oil palm trees, healthy oil palm trees, forest, background, road and others in case of UAV image. The training areas were defined from field survey data and base map from google earth. Each type of data class from field data was calculated in the statistics.

Accuracy Assessment

An accuracy assessment from the supervised classification of the image was based on the reference data with a confusion matrix (Congalton, 1991; Nuthammachot *et al.*, 2019). The field trip data were selected samples of raster or Regions of Interest (ROIs). Then the predicted class from the satellite and UAV images were extracted from the SVM classification method based on the ROIs. Overall accuracy, producer's accuracy, user's accuracy and kappa coefficient of agreement (κ) were performed to determine the accuracy of the diseased and healthy oil palm trees map.

Validation

Validation is generally used to assess the performance of a model (Lu *et al.*, 2011; 2016). The VARI is a vegetation index for estimating vegetation fractions quantitatively with only the visible range of the spectrum (ESRI, 2021). The two sample data groups VARI of UAV and VARI of Sentinel-2 data were selected in each area. The relationship between two variables was estimated to validate the model using linear regression. A scatterplot graph is a powerful tool for defining the strength of the relationship between two variables. The high coefficient of determination R^2 value determines the reliability of the model (Che *et al.*, 2021; Norouzian *et al.*, 2021; Robson *et al.*, 2017; Zhao *et al.*, 2021).

RESULTS

Vegetation indices

Table 3 shows the result of the linear regression analysis between the vegetation indices from Sentinel-2 images values and VARI indices from UAV. It was found that the r-values of vegetation indices ranged from 0.05 to 0.69 and the coefficient of determination (R^2) varied between 0.01 and 0.48 for the healthy oil palm trees area. For the diseased oil palm trees area, the r-values were between 0.07 and 0.82 and R^2 values were between 0.01 and 0.68. Similarly, the r-values of the mixed oil palm trees area were between 0.12 and 0.66 and R^2 values were between 0.02 and 0.44. For the healthy oil palm trees area, NDVI indices gave the best performance (R^2 = 0.48 and r = 0.69). RVI, NDI45, MSAVI, GNDVI and NDVI indices showed a substantial level while the MTCI showed a trivial level of performance. In the case of the diseased oil palm trees area, the RVI was the best performing index (R^2 = 0.68 and r = 0.82) followed by NDVI, MSAVI, NDI45, GNDVI and MTCI. For the mixed oil palm trees area, MSAVI was the best performing index (R^2 = 0.44 and r = 0.66) followed by NDVI, RVI, GNDVI, NDI45 and MTCI.

Support Vector Machine Classification and Accuracy Assessment

The results from the SVM algorithm are presented in *Figures 3, 4* and *5*. In these figures, the location of the healthy and diseased oil palm trees, which was recorded during the field survey as ground truth data, is indicated by circles at the centre of each oil palm tree. For the accuracy assessment, producer's accuracy, user's accuracy, and kappa coefficient were calculated through an error matrix. The results for disease classification of the Sentinel-2 image indicated an overall accuracy of 64.16% and a kappa coefficient of 0.40 while for UAV image an overall accuracy of 65.61% and a kappa coefficient of 0.55 was calculated. Moreover, the overall accuracy of healthy classification was

TABLE 3. CORRELATION AND LINEAR REGRESSION BETWEEN VEGETATION INDICES FROM SENTINEL-2 DATA AND VARI FROM UAV DATA

Indices	Healthy oil palm trees area		Diseased oil palm trees area		Mixed oil palm trees area	
	R^2	r	R^2	r	R^2	r
RVI	0.47	0.68*	**0.68**	0.82*	0.36	0.60*
NDI45	0.34	0.58*	0.42	0.65*	0.03	0.18*
MSAVI	0.43	0.66*	0.55	0.74*	**0.44**	0.66*
GNDVI	0.29	0.54*	0.29	0.54*	0.17	0.41*
MTCI	0.01	0.05*	0.01	0.07*	0.02	0.12*
NDVI	**0.48**	0.69*	0.67	0.82*	0.36	0.60*

Note: * - Refer to a significant correlation at 0.05 level.

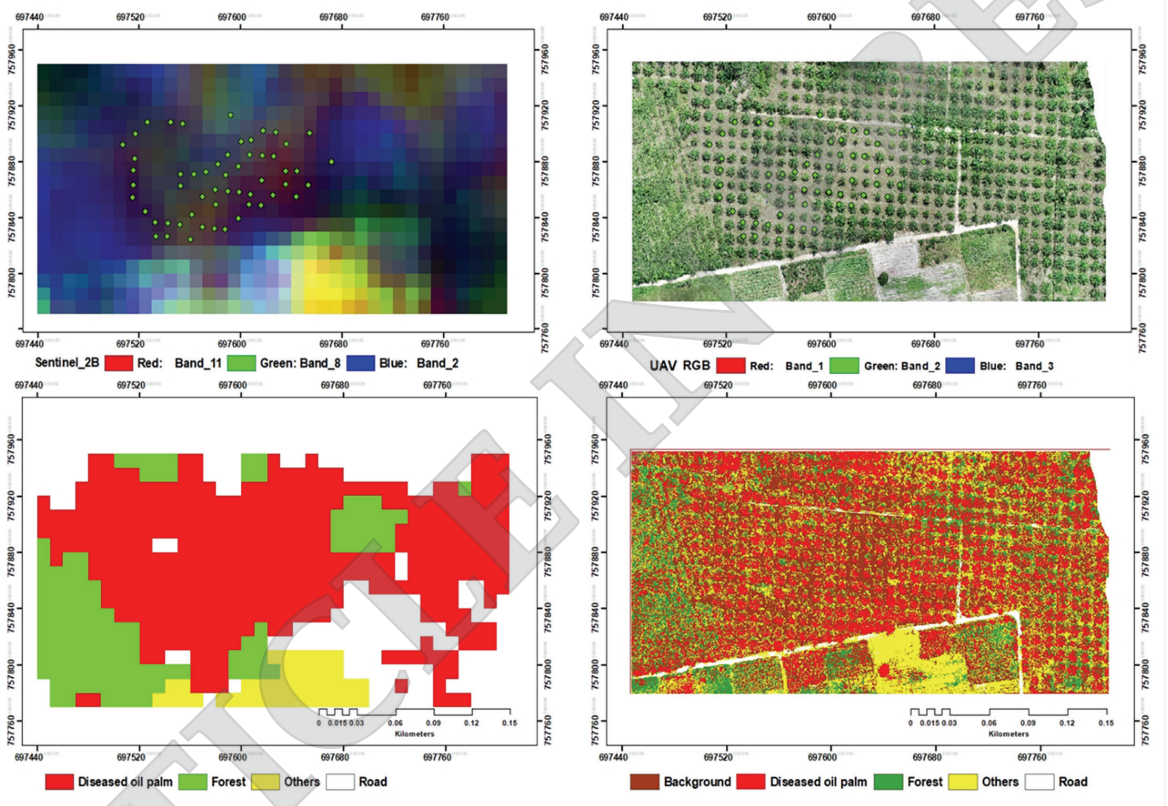

Figure 3. Identification of diseased oil palms planted area by SVM Classification.

72.97% and a kappa coefficient of 0.56 was shown in the case of the Sentinel-2 image while for UAV data overall accuracy of 76.77% and a kappa coefficient of 0.68 were estimated. For the mixed oil palm tree area, the overall accuracy was 50.00% and the kappa coefficient was 0.37 while UAV data had an overall accuracy of 67.22% and a kappa coefficient of 0.43 was found.

Validation

Figure 6 presents the results of the correlation between the VARI from Sentinel-2 satellite data and the VARI from UAV imagery. Simple linear regression and R^2 values are used to develop and validate this model. For a healthy oil palm field, the R^2 value is 0.61 so it means that 61.00% of VARI of Sentinel-2 could be explained by VARI of UAV. Moreover, it gave the highest R^2 value than others from diseased and mixed oil palm fields (R^2 = 0.58 and 0.19). It was found that the healthy oil palm tree area is the most reliable model while the mixed oil palm tree area is the least reliable model.

Spectral Response of Healthy and Diseased Oil Palm Trees using Sentinel-2 Satellite Image

The diseased oil palm trees have been observed on a regional scale. The results from this study indicate the potential of Sentinel-2 image for

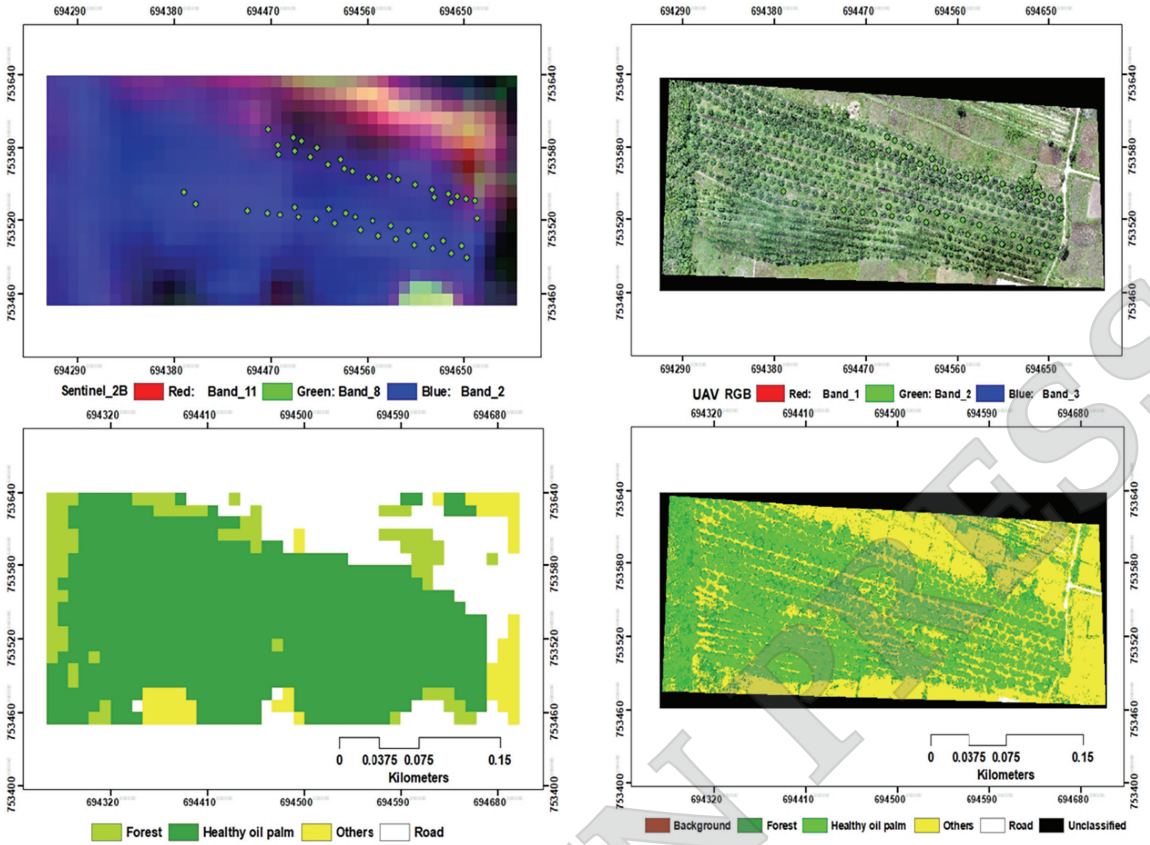

Figure 4. Identification of healthy oil palms planted area by SVM Classification.

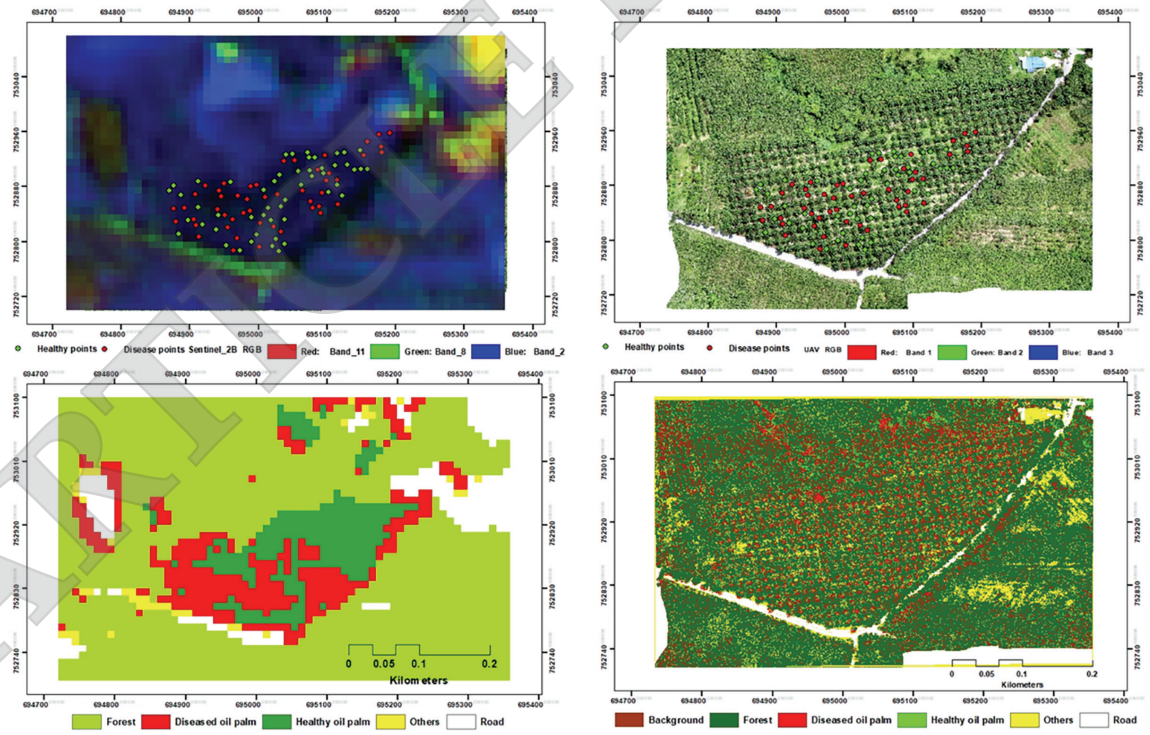

Figure 5. Identification of mixed oil palms planted area by SVM Classification.

accurately mapping diseased, healthy and mixed oil palm plantations in Chana district, Songkhla province, Thailand. The vegetation indices NDVI, RVI and MSAVI consistently produced the strongest relationship to the measured diseased, healthy and mixed oil palm parameters. This result indicates that variations in the oil palm canopy are sensitive to measure with the NIR and Red spectral bands,

a finding which is also confirmed by other studies (Malinee *et al.*, 2021; Noor, 2016). Therefore, it follows that the spectral signatures of healthy and diseased oil palm trees can be obtained from Sentinel-2 imagery. Healthy oil palm trees show a higher reflectance in the NIR range of the spectrum (band 6: 740.5 nm, band 7: 782.8 nm, band 8: 832.8 nm and band 8A: 864.7 nm) compared to diseased oil palm trees because the trees were generally greener, with higher chlorophyll content, leading to greater reflection (*Figure 7*).

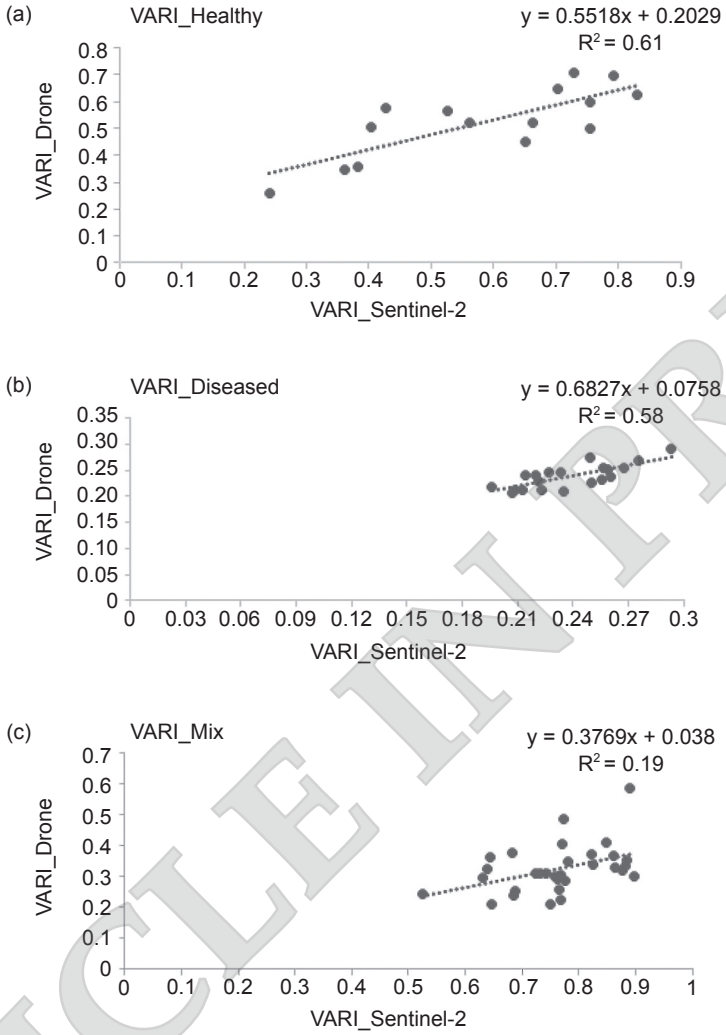

Figure 6. Scatter plot of VARI from Sentinel-2 satellite data and VARI from UAV imagery for the (a) healthy oil palm tree area, (b) diseased oil palm tree area and (c) mixed oil palm tree area.

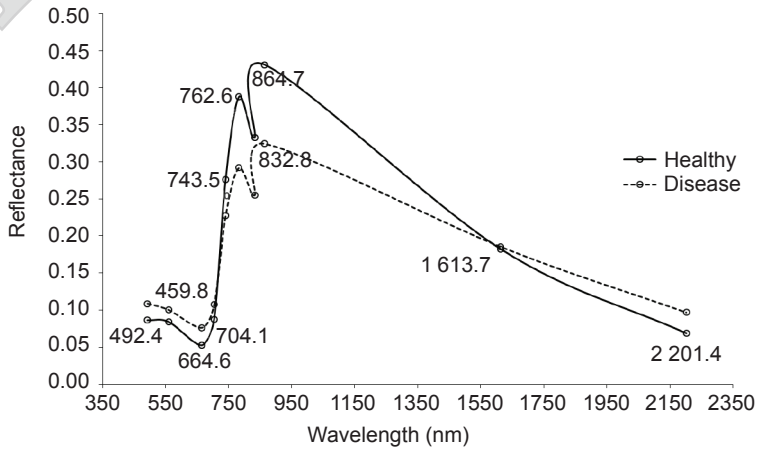

Figure 7. Spectral response of the healthy and diseased oil palm tree samples derived from the Sentinel-2 satellite image.

DISCUSSION

According to the accuracy of Sentinel-2 satellite classification of the two classes of diseased and healthy oil palm trees areas, the error matrix of the SVM classification was estimated. The results of this study show that the overall accuracy is 72.97% and the kappa coefficient is 0.56 (56.00%) in healthy oil palm planted areas and 64.16% and the kappa coefficient is 0.40 (40.00%) in diseased oil palm planted areas while the overall accuracy (50.00%) and the kappa coefficient (0.37) of mixed oil palm planted area are lower than others. The reason is that it is difficult to discriminate between the canopy of healthy and diseased oil palm trees using the medium satellite image. Compared with the results of UAV image, the overall accuracy and kappa coefficient values are higher than the results from Sentinel-2 data in the healthy, diseased oil palm tree and mixed oil palm tree areas. Furthermore, Santoso *et al.* (2017) classified oil palm disease using QuickBird satellite data. The overall accuracy (91.00%) is higher than our result. Also, Malinee *et al.* (2021) classified oil palm disease and provided an overall accuracy of 85.98%, and the kappa coefficient of 0.71 (71.00%) while our result of mixed oil palm trees is lower than their results. It is a fact that the UAV imagery, QuickBird and WorldView-2 satellite images have higher resolution than the Sentinel-2 satellite image.

CONCLUSION

The main finding of this study indicates that the SVM classification yielded satisfactory results for discriminating between plants and other objects in the case of healthy and diseased oil palm planted areas using Sentinel-2 satellite and UAV images. The results showed that the overall accuracy and kappa coefficient of the Sentinel-2 satellite data were 72.97% and 0.56 in the healthy oil palm trees region and 64.16 % and 0.55 in the diseased oil palm trees area. Moreover, UAV data overall accuracy was 76.77% and the kappa coefficient was 0.68 for the healthy oil palm trees area and 65.61% and a kappa coefficient of 0.55 was calculated for the diseased oil palm trees area. However, it is not easy to classify diseased and healthy oil palm trees in the mixed oil palm area (50.00% and 0.37). Future efforts to improve the methodology proposed are suggested to focus on obtaining more precise estimates. First, the satellite image is required to be of a very high radiometric resolution such as a hyperspectral image. Secondly, the UAV should have the NIR or hyperspectral sensor to detect or monitor diseased plants and can calculate narrowband vegetation indices with high accuracy. Finally, other physical parameters, such as nutrition analysis of the oil palm leaf, should be considered as it also contributes to disease infection.

ACKNOWLEDGEMENT

The authors deeply appreciate the support and received funding from Prince of Songkla University (Grant No: ENV6302159S), Research and Development Office, Prince of Songkla University, Thailand.

REFERENCES

Askar; Nuthammachot, N; Phairuang, W; Wicaksono, P and Sayektiningsih, T (2018). Estimating above ground biomass on private forest using Sentinel-2 imagery. *J. Sens., 2018:* 6745629. DOI: 10.1155/2018/6745629.

Chaware, R; Karpe, R; Pakhale, P and Desai, S (2017). Detection and recognition of leaf disease using image processing. *Int. J. Comput. Sci. Eng., 7(5)*: 11964-11967.

Che, X; Zhang, H K and Liu, J (2021). Making Landsat 5, 7 and 8 reflectance consistent using MODIS nadir-BRDF adjusted reflectance as reference. *Remote Sens. Environ., 262*:112517. DOI: 10.1016/j.rse.2021.112517.

Cheng, Y; Yu, L; Xu, Y; Liu, X; Lu, H; Cracknell, A P; Kanniah, K and Gong, P (2018). Towards global oil palm plantation mapping using remote-sensing data. *Int. J. Remote Sens., 39(18)*: 5891-5906. DOI: 10.1080/01431161.2018.1492182.

Cheng, Y; Yu, L; Xu, Y; Lu, H; Cracknell, A P; Kanniah, K and Gong, P (2019). Mapping oil palm plantation expansion in Malaysia over the past decade (2007-2016) using ALOS-1/2 PALSAR-1/2 data. *Int. J. Remote Sens., 40(19)*: 7389-7408. DOI:10.1080/01431161.2019.1580824.

Chong, K L; Kanniah, K D; Pohl, C and Tan, K P (2017). A review of remote sensing applications for oil palm studies. *Geo. Spat. Inf. Sci., 20(2)*: 184-200. DOI: 10.1080/10095020.2017.1337317.

Congalton, R G (1991). A review of assessing the accuracy of classifications of remotely sensed data. *Remote Sens. Environ., 37(1):* 35-46. DOI: 10.1016/0034-4257(91)90048-B.

Delegido, J; Verrelst, J; Alonso, L and Moreno, J (2011). Evaluation of sentinel-2 red-edge bands for empirical estimation of green LAI and chlorophyll content. *Sensors., 11(7)*: 7063-7081. DOI: 10.3390/s110707063.

DJI (2017). Phantom 4: User Manual V1, 2016-11. https://dl.djicdn.com/downloads/phantom_4/en/Phantom_4_User_Manual_en_v1.0.pdf, accessed on 7 July 2021.

ESRI (2021). ArcGIS Pro. https://pro.arcgis.com/en/pro-app/latest/arcpy/image-analyst/vari.html, accessed on 17 June 2021.

European Space Agency (ESA) (2021). Sentinel Online. https://sentinel.esa.int, accessed on 17 July 2021.

European Space Agency (ESA) (2015). Sentinel Online (Sentinel-2). https://sentinel.esa.int/web/sentinel/missions/sentinel-2, accessed on 17 July 2021.

Gitelson, A A; Kaufman, Y J and Merzlyak, M N (1996). Use of a green channel in remote sensing of global vegetation from EOS-MODIS. *Remote Sens. Environ., 58(3)*: 289-298. DOI: 10.1016/S0034-4257(96)00072-7.

Izzuddin, M A; Nisfariza, M N; Ezzati, B; Idris, A S; Steven, M D and Boyd, D (2018). Analysis of airborne hyperspectral image using vegetation indices, red edge position and continuum removal for detection of *Ganoderma* disease in oil palm. *J. Oil Palm Res., 30*: 416-428. DOI: 10.21894/jopr.2018.0037.

Kamal, M M; Masazhar, A N I and Rahman, A (2018). Classification of leaf disease from image processing technique. *Indones. J. Electr. Eng., 10(1)*: 191-200. DOI: 10.11591/ijeecs.v10.i1.

Lu, D; Batistella, M; Moran, E; Hetrick, S; Alves, D and Brondizio, E (2011). Fractional forest cover mapping in the Brazilian Amazon with a combination of MODIS and TM images. *Int. J. Remote Sens., 32(22)*: 7131-7149. DOI: 10.1080/01431161.2010.519004.

Lu, D; Chen, Q; Wang, G; Liu, L; Li, G and Moran, E (2016). A survey of remote sensing-based above ground biomass estimation methods in forest ecosystems. *Int. J. Digit. Earth., 9(1)*: 63-105. DOI: 10.1080/17538947.2014.990526.

Malinee, R; Stratoulias, D and Nuthammachot, N (2021). Detection of oil palm disease in plantations in Krabi Province, Thailand with high spatial resolution satellite imagery. *Agric., 11(3)*: 251. DOI: 10.3390/agriculture11030251.

Masazhar, A N I and Kamal, M M (2017). Digital image processing technique for palm oil leaf disease detection using multiclass SVM classifier. *In 2017 IEEE 4th International conference on smart instrumentation, measurement and application (ICSIMA)*. p. 1-6.

Naher, L; Yusuf, U K; Ismail, A; Tan, S G and Mondal, M M A (2013). Ecological status of *Ganoderma* and basal stem rot disease of oil palms (*Elaeis guineensis* Jacq.). *Aust. J. Crop Sci., 7(11)*: 1723-1727.

Noor, N M (2016). *El uso de sensores remotos para detectar la infección por* Ganoderma. *Revista Palmas., 37*:140-150.

Norouzian, M A; Bayatani, H and Alavijeh, M V (2021). Comparison of artificial neural networks and multiple linear regression for prediction of dairy cow locomotion score. *Vet. Res. Forum., 12(1)*: 33-37. DOI: 10.30466/vrf.2019.98275.2346.

Nuthammachot, N and Stratoulias, D (2019). Fusion of Sentinel-1A and Landsat-8 images for improving land use/land cover classification in Songkla province, Thailand. *Appl. Ecol. Environ. Res., 17(2)*: 3123-3135. DOI: 10.15666/aeer/1702_31233135.

Pałaś, K W and Zawadzki, J (2020). Sentinel-2 imagery processing for tree logging observations on the Białowieża forest world heritage site. *Forests., 11(8)*: 857. DOI: 10.3390/f11080857.

Qi, J; Chehbouni, A; Huerte, A R; Kerr, Y H and Sorooshian, S (1994). A modified soil adjusted vegetation index. *Remote Sens. Environ., 48(2)*: 119-126. DOI: 10.1016/0034-4257(94)90134-1.

Robson, A; Rahman, M M and Muir, J (2017). Using worldview satellite imagery to map yield in avocado (*Persea americana*): A case study in Bundaberg, Australia. *Remote Sens., 9(12)*: 1223. DOI10.3390/rs9121223.

Santoso, H; Gunawan, T; Jatmiko, R H; Darmosarkoro, W and Minasny, B (2011). Mapping and identifying basal stem rot disease in oil palms in North Sumatra with QuickBird imagery. *Precis. Agric., 12(2)*: 233-248. DOI: 10.1007/s11119-010-9172-7.

Santoso, H; Tani, H and Wang, X (2017). Random forest classification model of basal stem rot disease caused by *Ganoderma boninense* in oil palm plantations. *Int. J. Remote Sens., 38(16)*: 4683-4699. DOI: 10.1080/01431161.2017.1331474.

Tucker, C J (1979). Red and photographic infrared linear combinations for monitoring vegetation. *Remote Sens. Environ., 8(2)*: 127-150. DOI: 10.1016/0034-4257(79)90013-0.

Yusoff, N M; Muharam, F M and Khairunniza-Bejo, S (2017). Towards the use of remote-sensing data for monitoring of abandoned oil palm lands in Malaysia: A semi-automatic approach. *Int. J. Remote Sens., 38(2)*: 432-449. DOI: 10.1080/01431161.2016.1266111.

Zhang, K; Liu, X; Ma, Y; Wang, Y; Cao, Q; Zhu, Y; Cao, W and Tian, Y (2021). A new canopy chlorophyll index-based paddy rice critical nitrogen dilution curve in Eastern China. *Field Crops Res., 266*: 108139. DOI: 10.1016/j.fcr.2021.108139.

Zhao, Y; Liu, X; Wang, Y; Zheng, Z; Zheng, S; Zhao, D and Bai, Y (2021). UAV-based individual shrub above ground biomass estimation alibrated against terrestrial LiDAR in a shrub-encroached grassland. *Int. J. Appl. Earth Obs. Geoinf., 101*:102358. DOI: 10.1016/j.jag.2021.102358.